G-Quadruplexes

DOI: 10.1002/ange.201306230

Real-Time Optical Detection of Stabilized Artificial G-Quadruplexes Under Confined Conditions

*Bogdan George Rusu, Frédérique Cunin, and Mihail Barboiu**

Constitutional self-assembly provides an evolutional approach for the generation of functional supramolecular systems through the implementation of reversible exchange between different complex architectures of various functionalities.[1–4] A representative example is the generation of H-bonded guanosine (G)-quadruplexes through cation templating, which may embody an important constitutional (spatial and interactional) reorganization of G-networks by dynamically exchanging between G-ribbons and cation-stabilized macrocyclic G-quartets or tubular G-quadruplexes (Figure 1 a).[5a] Although they were already discovered in the 1960s,[5b] the application of artificial G-quadruplexes as ion channels[6] and the direct quantification of natural G-quadruplexes in human cells have only recently been studied extensively.[6] Liposomes,[7] surfaces,[8] dynamers,[9] hybrid materials,[10,11] and mesoporous silica[12] have been used as scaffolding matrices to stabilize and to orient the anisotropic directional G-mesophases. They are reminiscent of other supramolecular pore-confined systems[13,14] or DNA-modified surfaces.[15,16]

Among confining matrices, single-layer thin films of mesoporous silicon (pSi), multilayer Bragg reflectors, or Rugate filters can be easily obtained by electrochemical etching (Supporting Information, Figure S1 a). The single-layer films display properties suitable for optical interferometry, and well-resolved Fabry–Perot fringes are obtained in the pSi reflectivity interference spectrum.[17,18] Numerous optical (bio)sensors have been developed using reflective interferometric Fourier transform spectroscopy (RIFTS).[19–22] Rugate filters of pSi multilayers that feature a sinusoidal variation of the depth mesoporosity and a strong peak in their reflectivity spectrum reflect a single color without a Fourier transform operation.[22]

We hypothesized that, under pSi confinement, the transformation between the G-ribbon and G-quadruplex phases of distinct molecular packing density would result in a change in the refractive index of the pSi structure (Figure 1 b), which can be detected as the corresponding shift of the effective optical-thickness value in its fast Fourier interference pattern (Figure 1 c).

Herein, *O*-triacetylguanosine (AcG) and cation building blocks have been used to stabilize the AcG_n-ribbons and AcG-quadruplexes under confinement within pSi. Their formation under confined conditions can be detected with single-layer films (RIFTS) or Rugate filters by monitoring the real-time variation of the effective optical thickness in the pSi host matrix and direct color changes, respectively.

G-quadruplexes were prepared from AcG and Na^+, K^+, or Ba^{2+} triflates in acetonitrile. A weak Cotton effect was observed in the CD spectrum of AcG, which may be ascribed to a very fast exchange between the twisted unstructured G-quadruplex with ribbons in solution (Supporting Information, Figure S2 a). After addition of Na^+, K^+, or Ba^{2+} (0.25 equiv), the CD spectra closely resembled the calculated spectra of chiral twisted G-quadruplexes, with adjacent G-quartets having opposite polarities (Supporting Information, Figure S2 a).[23,24] The spectra displayed the expected negative (Na^+, K^+) and positive (Ba^{2+}) Cotton effects, with a zero-crossing at $\lambda = 300$ nm in the region of the AcG chromophore. Evidence for H-bonding and cation binding was obtained from the shifts in the vibrational band of $\nu_{C=O,G}$ from 1700 to 1680 cm^{-1}, which was observed in the FTIR spectra of G-quadruplexes, while the $\nu_{C=O}$ band of external acetyl moieties at 1750 cm^{-1} did not shift (Supporting Information, Figure S2 b).

Porous silicon films were prepared by anodic etching of B-doped crystalline silicon in an ethanolic solution of hydrofluoric acid (HF) at various constant current densities of 2–30 mA cm^{-2}. Scanning electron microscopy (SEM) of the pSi surface (Supporting Information, Figure S3) showed mesopores with a diameter of approximately 7–26 nm, which increases with higher current densities as expected. The pSi mesopores provide a large surface area for the confinement of G-ribbons and G-quadruplexes that are considered to have a length of 1 nm and a diameter of 3.5 nm, respectively.[8–10] The freshly etched hydride-terminated pSi was rendered hydrophobic by hydrosilylation with hexadecene. Then, the AcG_n ribbons or pre-formed AcG_4Na^+, AcG_4K^+, and AcG_4Ba^{2+} quadruplexes were confined or generated in situ upon continuous addition of the corresponding salt solutions to an AcG_n–hexadecane–pSi sample mounted in a flow cell (Supporting Information, Figure S1 b). Upon sequestration within the pSi pores, almost all of the vibrational FTIR bands were shifted to higher frequencies compared with the unconfined G-systems, which is reminiscent of the more rigid vibrational modes under confined conditions (Support-

[*] B. G. Rusu, Dr. M. Barboiu
Adaptive Supramolecular Nanosystems Group
Institut Européen des Membranes, ENSCM-UMII-UMR-CNRS 5635
Place Eugène Bataillon CC047, 34095 Montpellier (France)
E-mail: mihail-dumitru.barboiu@univ-montp2.fr
B. G. Rusu
Alexandru Ioan Cuza University of Iasi, Faculty of Physics
Bd. Carol I no.11, 700506 (Iasi Romania)
B. G. Rusu, Dr. F. Cunin
Institut Charles Gerhardt Montpellier (ICGM), UMR 5253 CNRS/ENSCM/Université de Montpellier II
8 rue de l'Ecole Normale, F-34296 Montpellier (France)

Supporting information for this article is available on the WWW under http://dx.doi.org/10.1002/anie.201306230.

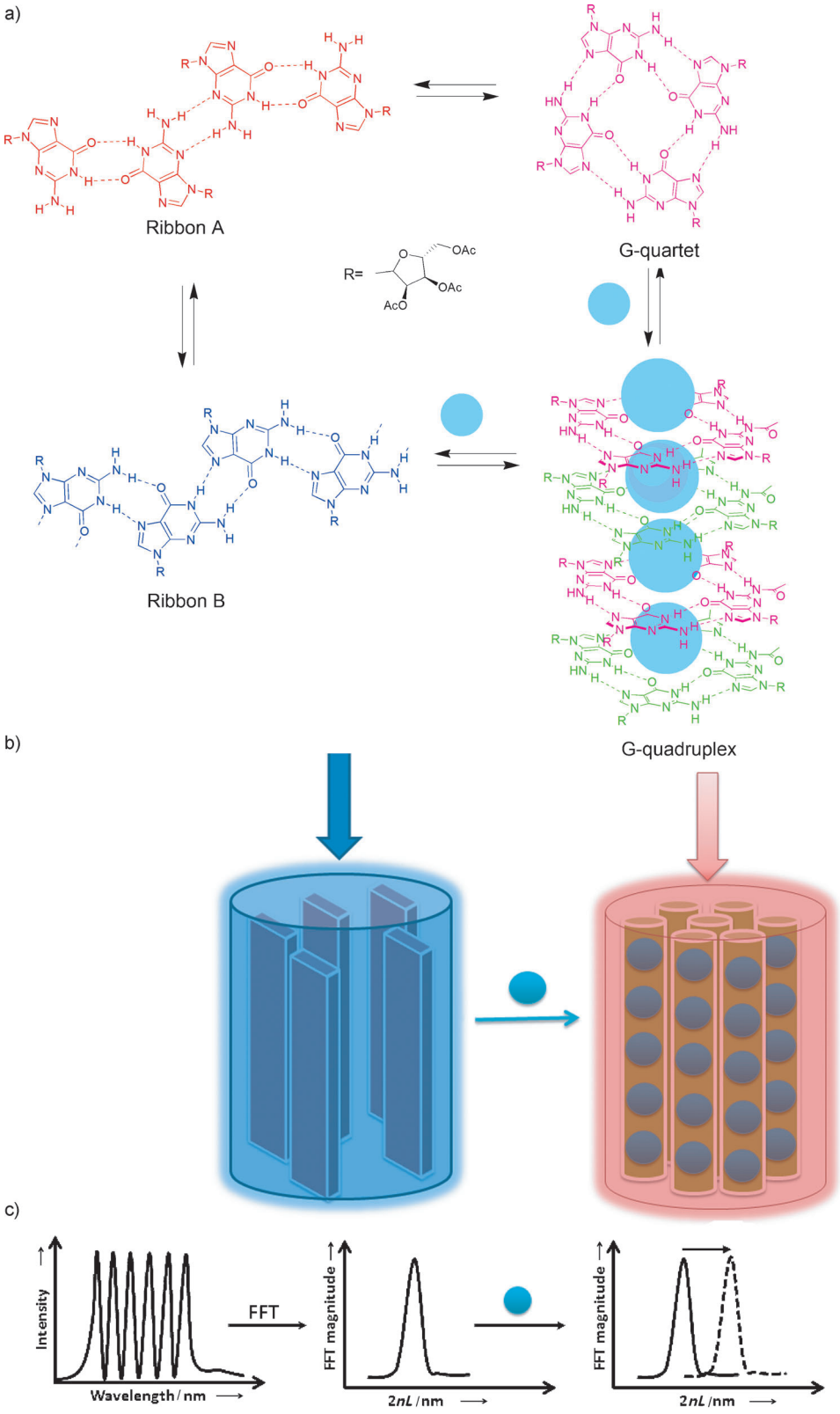

Figure 1. a) Dynamic exchange between supramolecular architectures of G-ribbons, G-quartets, or G-quadruplexes in the presence of ionic chemical effectors (●). b) Dynamic constitutional confinement of ribbon-type and cylindrical G-quadruplex architectures of different molecular packing density. c) A change in refractive index results, which is detected as the corresponding shift of $2nL$ (effective optical thickness) in the interference pattern of the hybrid pSi film.

ing Information, Figure S4). The X-ray powder diffraction (XRPD) patterns of the AcG powder entailed well-resolved peaks that are reminiscent of the co-existence of linear[25] and zigzag[26] ribbons **B** (Figure S5). The preferential formation of ribbons **B** is governed by strong interactions between the three hydrophobic acetyl groups that induce the formation of the more compact architecture to increase the overall stability of the system, as previously observed for similar systems.[27]

The confinement of G-systems within the hexadecane–pSi films (7–26 nm) was then investigated using RIFTS (Supporting Information, Figure S2b).[28] The addition of solutions of AcG_n and of preformed AcG_4Na^+, AcG_4K^+, and AcG_4Ba^{2+} induced a rapid increase in optical thickness-($\Delta 2nL$), which was followed by a plateau that is attributed to non-covalent confinement and then saturation of the pores by the G-systems (Figure 2). The increase in $\Delta 2nL$ was higher for the bigger pores, which corresponds to larger amounts of confined G-species (Supporting Information, Figure S6). The AcG_n ribbons generated a larger red-shift in the effective optical thickness than the cationic AcG-quadruplexes because of their different molecular packing densities. Then, the formation of AcG-quadruplexes by the addition of K^+ or Ba^{2+} solutions to a porous pSi system saturated with AcG_n was monitored. Astonishingly, the value $\Delta 2nL$ shifted back to its initial value, which indicates complete removal of the confined AcG_n from the pores, along with the formation of AcG_4K^+ and AcG_4Ba^{2+} in acetonitrile solution (Figure 2b,c).

When performed a month later, the same experiment on hexadecane–pSi samples that

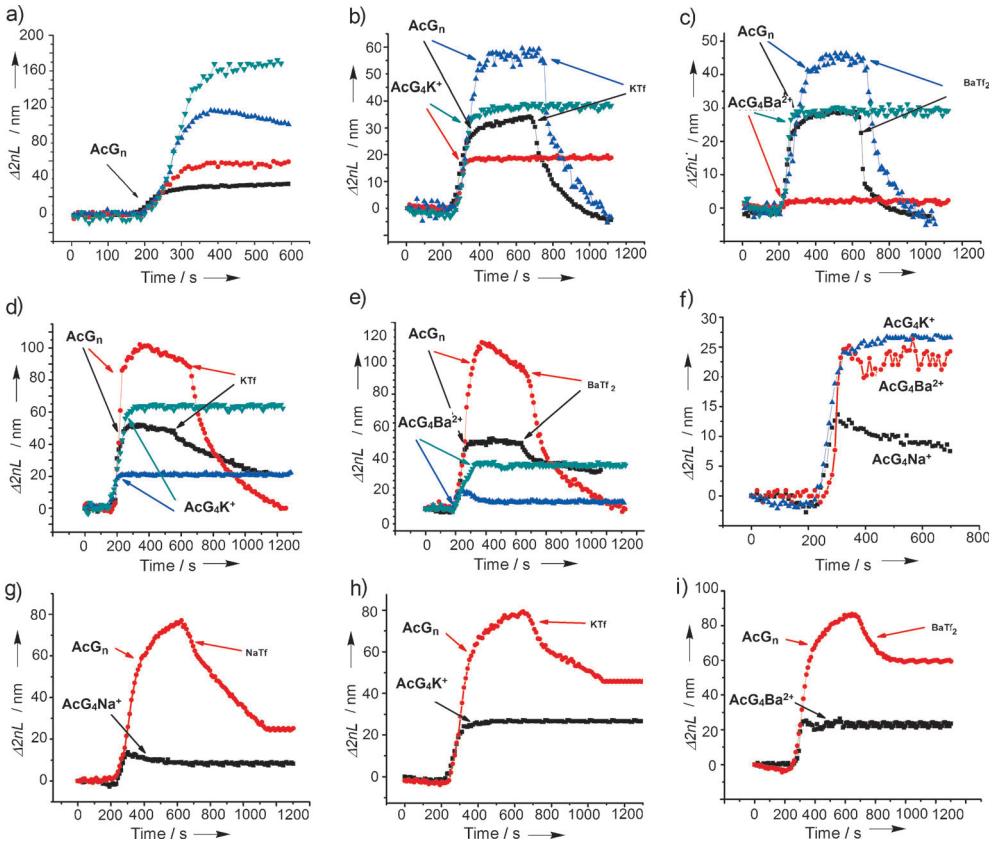

Figure 2. Variation of the effective optical thickness as a function of time. a) $\Delta 2nL = f(t)$ for hexadecane-modified pSi samples prepared at different current densities (2–30 mA cm^{-2}) and exposed to AcG_n ribbons. b–e) $\Delta 2nL = f(t)$ for hexadecane–pSi samples prepared at 2 and 5 mA cm^{-2}, presaturated with AcG_n, and exposed to b) K^+ and c) Ba^{2+} cations; d, e) one-month old hexadecane–pSi samples, presaturated with AcG_n, and exposed to d) K^+ and e) Ba^2 cations. f) $\Delta 2nL = f(t)$ for pSi-COO^- samples prepared at 2 mA cm^{-2} and exposed to preformed AcG_4Na^+, AcG_4K^+, and AcG_4Ba^{2+}. g–i) $\Delta 2nL = f(t)$ for pSi-COO^- samples prepared at 2 mA cm^{-2}, presaturated with AcG_n, and exposed to g) Na^+, h) K^+, and i) Ba^{2+} cations. Traces for preformed AcG_4Na^+, AcG_4K^+, and AcG_4Ba^{2+} are shown in each graph (b–e) and (g–i) for comparison. ■ = 2 mA; ● = 5 mA; ▲ = 10 mA; ▼ = 30 mA.

were aged and partially oxidized (by ambient air) revealed a different behavior in the RIFTS experiment for low pore-diameter pSi films (2 and 5 mA cm^{-2}) that present a better potential for interaction and stabilization of their inner-pore surfaces with the G-systems. These results suggest that the partially hydrophilic/charged Si–OH/Si–O^- aged pore surface plays a role in the stabilization of the positively charged AcG_4K^+ and AcG_4Ba^{2+} when formed in situ in pSi (Figure 2 d,e). For this reason, we then prepared pSiCOO^- samples (2 mA cm^{-2}) by the hydrosilylation of hexadecenoic acid onto a pSi film. Introduction of preformed positively charged AcG_4K^+ and AcG_4Ba^{2+} to the pSi-COO^- films induced a rapid red-shift to higher saturation values of $\Delta 2nL$, which could be attributed to the increased charge compensation of confined G-quadruplexes (Figure 2 f). The real-time formation of G-quadruplexes from saturated confined AcG_n that was exposed to the Na^+, K^+, or Ba^{2+} solutions showed a significant and timely blue-shift, which corresponds to a slow equilibrium between AcG_n and the $AcGNa^+$, AcG_4K^+, or AcG_4Ba^{2+} species within the pSiCOO^- pores. The final value for the effective optical thickness was found to be higher than the value that could be reached when introducing preformed quadruplexes (Figure 2 g–i). In fact, the in situ formation of the quadruplexes from preloaded confined AcG_n ribbons of high packing density allowed an enhanced loading of the quadruplexes compared to when the quadruplexes were directly loaded. This confinement effect was more pronounced for AcG_4Ba^{2+} than for AcG_4K^+, and even less pronounced for AcG_4Na^+, as determined by the blue-shift values $\Delta 2nL$ of 27, 35, and 55 nm respectively. Indeed, it is known that in a series of quadruplexes, AcG_4Ba^{2+} is thermodynamically and kinetically more stable than AcG_4K^+, whereas AcG_4Na^+ is generally unstable.[12,29] Confinement and packing are assumed to be more favorable when the system is stabilized in one or the other conformation (linear ribbon or quadruplex), and when only limited exchange between those conformations occurs.

Finally, Rugate-filter pSi structures, which strongly reflect green light, were etched with a sinusoidal variation of current density (15–45 mA cm^{-2}) over time with a pore diameter of 5–30 nm and then functionalized with hexadecenoic acid (Supporting Information, Figure S7). They were exposed to acetonitrile solutions of $AcGNa^+$, AcG_4K^+, and AcG_4Ba^{2+}. In air, the green pSi-COO^- samples turned progressively orange/red, with a darker red observed for AcG_4K^+ and AcG_4Ba^{2+} (Figure 3). The incorporation of stable AcG_4Ba^{2+} and AcG_4K^+ was expressed by greater red-shifts of the Rugate peak in solution than for the peak observed for $AcGNa^+$ (Table 1; Supporting Information, Figure S8), as previously observed by RIFTS measurements (Figure 2 f). In fact, the red-shift that was measured for AcG_4Na^+ (44 nm) corresponded to the red-shift observed upon introduction of pure acetonitrile (46 nm; Supporting Information, Figure S8 a, b), which suggests the absence or a poor incorporation of unstable AcG_4Na^+ within the pores. Then, after slow evaporation of the solvent, the samples were dried under high vacuum for 48 hours. The pSi Rugate sample initially exposed to the $AcGNa^+$ solution turned back to its original green color as acetonitrile evaporated. In contrast, the pSi samples with AcG_4K^+ and AcG_4Ba^{2+} remained reddish or orange and were

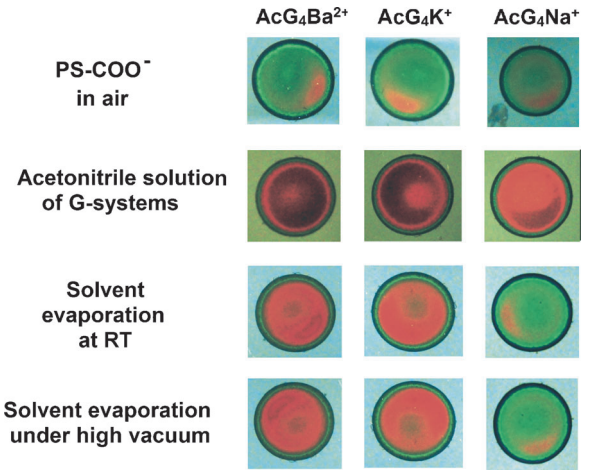

Figure 3. Photographs of pSi-COO^- Rugate films that display changes in optical color when exposed to acetonitrile solutions of AcG_n, AcG_4Na^+, AcG_4K^+, and AcG_4Ba^{2+}, after solvent evaporation at room temperature and under high-vacuum conditions to verify that the observed effects were not only related to solvent evaporation.

Table 1: Rugate peaks of pSi-COO^- multilayer films.[a]

G-System	Wavelength of the Rugate peaks[b] [nm]		
	AcG_4Ba^{2+}	AcG_4K^+	AcG_4Na^+
pSi-COO^- (air)	539	562	555
Acetonitrile solution of the G-system	622 (+83)	625 (+63)	599 (+44)
After solvent evaporation under high vacuum	597 (+58) orange/ red	575 (+13) yellow/ orange	562 (+7) green

[a] Rugate peaks for pSi-COO^- multilayer films in air, after immersion into acetonitrile solutions of the G-systems, and after evaporation under high-vacuum conditions. [b] The shifts of the Rugate peak for the confined G-systems (solution/solvent evaporation) are given in brackets, as a reference to the pSi-COO^- multilayer films in air.

stable for weeks in the absence of perturbing factors. The differences in red-shift observed for AcG_4K^+ and AcG_4Ba^{2+} of 63 and 83 nm, respectively (Supporting Information, Figure S8c, d), were in agreement with the expected stabilities of the two complexes.

Our findings show a novel interesting strategy to stabilize and to detect artificial G-quadruplexes under confinement within scaffolding porous silicon pSi matrices. Moreover, these experiments highlight the potential of pSi optical systems to sense formation of the G-quadruplexes in real-time, and to allow discrimination between the structurally similar $AcGNa^+$, AcG_4K^+, and AcG_4Ba^{2+} quadruplexes; thus, these systems can give information on dynamic binding events of ion effectors under confined conditions. The reflective optical properties of the pSi material can be used for fine-selective sensing of artificial G-quadruplexes, and they can be correlated with the stability of the G-quadruplexes ($AcGNa^+ < AcG_4K^+ < AcG_4Ba^{2+}$). When G-quadruplexes infused into the pores, a change in the film color from green to red occurred, so that confinement and stabilization of G-quadruplexes, or the color of self-assembly, can be directly observed by eye.

Considering the simplicity of this strategy, applications for the detection of other self-assemblies or molecular recognition processes could be developed.

Received: July 17, 2013
Revised: August 27, 2013
Published online: October 2, 2013

Keywords: constitutional chemistry · G-quadruplexes · porous materials · self-assembly · silicon

[1] a) J.-M. Lehn, *Chem. Soc. Rev.* **2007**, *36*, 151 – 160; b) E. Moulin, G. Cormos, N. Giuseppone, *Chem. Soc. Rev.* **2012**, *41*, 1031 – 1049; c) K. S. Mali, J. Adisoejoso, E. Ghijsens, I. De Cat, S. De Freyter, *Acc. Chem. Res.* **2012**, *45*, 1309 – 1320; d) M. M. Safont-Sempere, G. Fernandez, F. Würthner, *Chem. Rev.* **2011**, *111*, 5784 – 5814; e) L. M. Salonen, M. Ellermann, F. Diederich, *Angew. Chem.* **2011**, *123*, 4908 – 4944; *Angew. Chem. Int. Ed.* **2011**, *50*, 4808 – 4842.
[2] "Constitutional Dynamic Chemistry": *Topics in Current Chemistry*, *Vol. 322* (Ed.: M. Barboiu), Springer, Berlin, **2012**.
[3] M. Barboiu, *Chem. Commun.* **2010**, *46*, 7466 – 7476.
[4] Y. M. Legrand, A. van der Lee, M. Barboiu, *Science* **2010**, *329*, 299 – 302.
[5] a) J. T. Davis, *Angew. Chem.* **2004**, *116*, 684 – 716; *Angew. Chem. Int. Ed.* **2004**, *43*, 668 – 698; b) M. Gellert, M. Lipsett, D. Davies, *Proc. Natl. Acad. Sci. USA* **1962**, *48*, 2013 – 2018.
[6] G. Biffi, D. Tannahill, J. McCafferty, S. Balasubramanian, *Nat. Chem.* **2013**, *5*, 182 – 186.
[7] M. S. Kaucher, W. A. Harrell, J. T. Davis, *J. Am. Chem. Soc.* **2006**, *128*, 38 – 39.
[8] A. Ciesielski, S. Lena, S. Masiero, G. P. Spada, P. Samori, *Angew. Chem.* **2010**, *122*, 2007 – 2010; *Angew. Chem. Int. Ed.* **2010**, *49*, 1963 – 1966.
[9] C. Arnal-Hérault, A. Banu, M. Michau, D. Cot, E. Petit, M. Barboiu, *Angew. Chem.* **2007**, *119*, 8561 – 8565; *Angew. Chem. Int. Ed.* **2007**, *46*, 8409 – 8413.
[10] C. Arnal-Hérault, M. Michau, A. Pasc, M. Barboiu, *Angew. Chem.* **2007**, *119*, 4346 – 4350; *Angew. Chem. Int. Ed.* **2007**, *46*, 4268 – 4272.
[11] a) S. Mihai, A. Cazacu, C. Arnal-Hérault, G. Nasr, A. Meffre, A. van der Lee, M. Barboiu, *New J. Chem.* **2009**, *33*, 2335 – 2343; b) S. Mihai, Y. Le Duc, D. Cot, M. Barboiu, *J. Mater. Chem.* **2010**, *20*, 9443 – 9448.
[12] S. Mihai, J. Dauthier, Y. Le Duc, A. El Mansouri, A. Mehdi, M. Barboiu, *Eur. J. Inorg. Chem.* **2012**, 5299 – 5304.
[13] A. Cazacu, Y. M. Legrand, A. Pasc, G. Nasr, A. van der Lee, E. Mahon, M. Barboiu, *Proc. Natl. Acad. Sci. USA* **2009**, *106*, 8117 – 8122.
[14] A. Cazacu, S. Mihai, G. Nasr, E. Mahon, A. van der Lee, A. Meffre, M. Barboiu, *Inorg. Chim. Acta* **2010**, *363*, 4214 – 4219.
[15] D. I. Rozkiewicz, W. Brugman, R. M. Kerkhoven, B. J. Ravoo, D. N. Reinhoudt, *J. Am. Chem. Soc.* **2007**, *129*, 11593 – 11599.
[16] D. I. Rozkiewicz, J. Gierlich, G. A. Burley, K. Gutsmiedl, T. Carrel, B. J. Ravoo, D. N. Reinhoudt, *ChemBioChem* **2007**, *8*, 1997 – 2002.
[17] C. Pacholski, M. Sartor, M. J. Sailor, F. Cunin, G. M. Miskelly, *J. Am. Chem. Soc.* **2005**, *127*, 11636 – 11645.
[18] V. S.-Y. Lin, K. Motesharei, K.-P. S. Dancil, M. J. Sailor, M. R. Ghadiri, *Science* **1997**, *278*, 840 – 843.
[19] S. Pace, B. Seantier, M. Belamie, N. Lautrédou, M. J. Sailor, P. E. Milhiet, F. Cunin, *Langmuir* **2012**, *28*, 6960 – 6969.

[20] C. Pacholski, C. Yu, G. M. Miskelly, D. Godin, M. J. Sailor, *J. Am. Chem. Soc.* **2006**, *128*, 4250 – 4252.
[21] S. Pace, R. B. Vasani, F. Cunin, N. H. Voelcker, *New J. Chem.* **2013**, *37*, 228 – 223.
[22] The maxima of the reflectivity interference spectrum are described by the Fabry – Perot equation, $m\lambda = 2nL$ (with m an integer, L = thickness of the film, n = average refractive index of the film, and λ = wavelength of incident light). The product $2nL$ refers to the effective optical thickness of the film; the refractive index is a composite value of the refractive index of the pSi film and the refractive index of the media confined within its pores. For details, see: M. J. Sailor, *Porous Silicon in Practice: Preparation, Characterization and Applications*, Wiley-VCH, Weinheim, **2011**.
[23] D. M. Gray, J.-D. Wen, C. W. Gray, R. Repges, C. Repges, G. Raabe, J. Fleischhauer, *Chirality* **2008**, *20*, 431 – 440.
[24] K. Hanabusa, M. Yamada, M. Kimura, H. Shirai, *Angew. Chem.* **1996**, *108*, 2086 – 2088; *Angew. Chem. Int. Ed. Engl.* **1996**, *35*, 1949 – 1951.
[25] C. C. Wilson, J. N. Low, P. Tollin, *Acta Crystallogr. Sect. C* **1985**, *41*, 1123.
[26] J. N. Low, C. C. Wilson, P. Tollin, S. N. Scrimgeour, *Acta Crystallogr. Sect. C* **1986**, *42*, 700.
[27] C. Arnal-Hérault, M. Barboiu, A. Pasc, M. Michau, P. Perriat, A. van der Lee, *Chem. Eur. J.* **2007**, *13*, 6792 – 6800.
[28] M. S. Salem, M. J. Sailor, F. A. Harraz, T. Sakka, Y. H. Ogata, *Phys. Status Solidi C* **2007**, *4*, 2073 – 2077.
[29] X. Shi, J. C. Fetiger, J. T. Davis, *J. Am. Chem. Soc.* **2001**, *123*, 6738 – 6739.

